Ion Concentration Polarization (ICP): From Ion Exchange Membranes to Micro/Nanofluidic Interconnect Devices - A Complete Review

D. Manikandan[1], Vishal V. R. Nandigana[2*]

[1]Department of Mechanical Engineering, Head of Membrane Technology and Deep Learning laboratory,
Fluid Systems Laboratory, Indian Institute of Technology Madras, Chennai 600036, India

[2]Founder of Blue Fma PVT LTD
*corresponding author: *nandiga[at]iitm.ac.in*, *https://bluefma.today*

Abstract: *In this review paper, we provide a detailed literature review on ion concentration polarization (ICP) phenomenon in ion exchange membranes (IEM) and in micro/ nanofluidic interconnect membranes. The ICP phenomenon has been studied for the last three decades and its orgin is yet to be clearly understood by the researchers. The review focuses on various mechanisms for ICP and overlimiting current phenomenon along with many applications utilizing the phenomenon of ICP.*

Keywords: Ion concentration polarization, Ion Exchange membranes, IEM, membrane technology, micro nanofluidics, micro nanofluidics applications, new industrial applications

1. Introduction

Ion exchange membranes (IEM) has many current applications in various industries including electrodialysis [1–4], hydrogen production/storage [5-10], energy generation as fuel cells [11–15], energy production/ storage/ packaging in battery applications. In IEM, the transport of ions/ fluids/ chemicals/ fuel/ solid-electrolytes/gases allows for the production/ storage/ packaging/ pipeline construction for applications in energy, safe drinking water supply and production, that is environmentally green friendly and compatible with the natural resources in its production and usage. The ion-selective nature of the IEM and compatibility with the fluid/solid/gases/mixture transport make the IEM conducive and approvable to use with natural resources in many of these applications in the present world time[16–30]. Fig. 1A shows an illustration on the arrangement of the ions inside an IEM sheet, where Fig. 1B shows, the ion arrangement inside a much bigger diameter/channel thickness sheets for applications needing ion selectivity, may find IEM sheets of dimensions in Fig 1A and applications necessiating energy applications may find IEM sheets of dimensions in Fig. 1B and higher. The integration of IEM sheets of nanometer size with IEM sheets/cells of microns size with them has carved a new field of research over the last decade called micro/nanofluidics membrane technology [31–44] with their success seen recently by researchers across world in the field of energy generation, ionic circuits, fluidic electronics, membrane technology for faster transport of solids/liquids/gases/mixtures of using membrane technology for pipeline construction industry. In this review, we focus on one of the most predominant observations of IEMs for all applications of membrane technology is ion concentration polarization, that over the last century efforts and research works till recent literature in 2021, helped membrane technology to maximize it's design and applications with maximum and best efficiency for energy, safe drinking water supply and production, that is environmentally green friendly and use in humankind of 2021 era.

2. Physics of IEM

IEM, like one in an anion exchange membrane (AEM) or like one in a cation exchange membrane (CEM) is shown in Fig. 2A. The physics of either an AEM/CEM is same where the ions move across the membrane, with depletion of both the cations and anions at one side of the membrane and enrichment of both cations and anions at the other side of the membrane. Fig. 2A shows when an electric field is applied normal to the CEM, anions are repelled from the cation-selective memebrane and attracted towards anode. At the same time, the cation-selective nature of the CEM results in blocking of anions from entering into the membrane and the cations become enriched at the cathode end since the cations cannot move towards the cathode and get adsorbed to the cathode. The formation of depletion and enrichment of ions on either side of IEM is called ion concentration polarization (ICP) [31–73]. The early works in the numerical/theoretical modeling works used a geometry focusing on the depletion region, owing to the limitations in the complexity of the theoretical and computational modeling of the IEM membrane technology states of matter and geometry designs of the IEM membrane technology. Fig. 2B shows the geometry and focus of the theory and computational modeling approaches on the depletion region, believing the depletion region, has the controlling and dominating resistance in the complete membrane technology of IEM circuit.
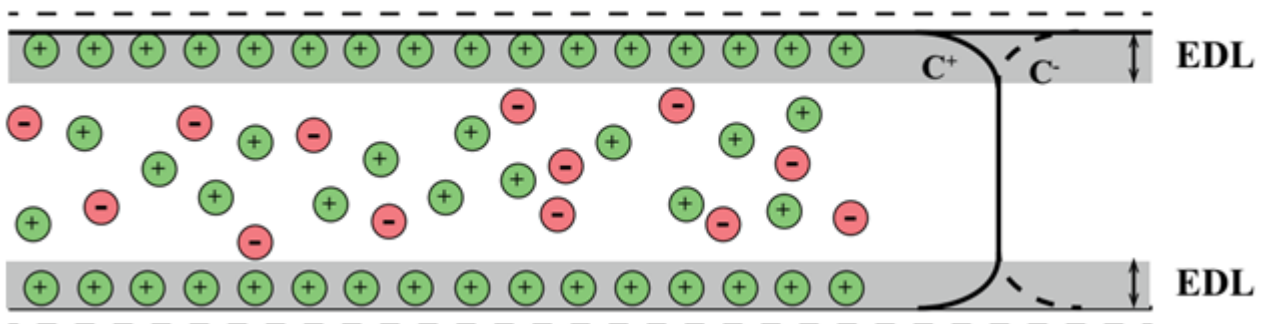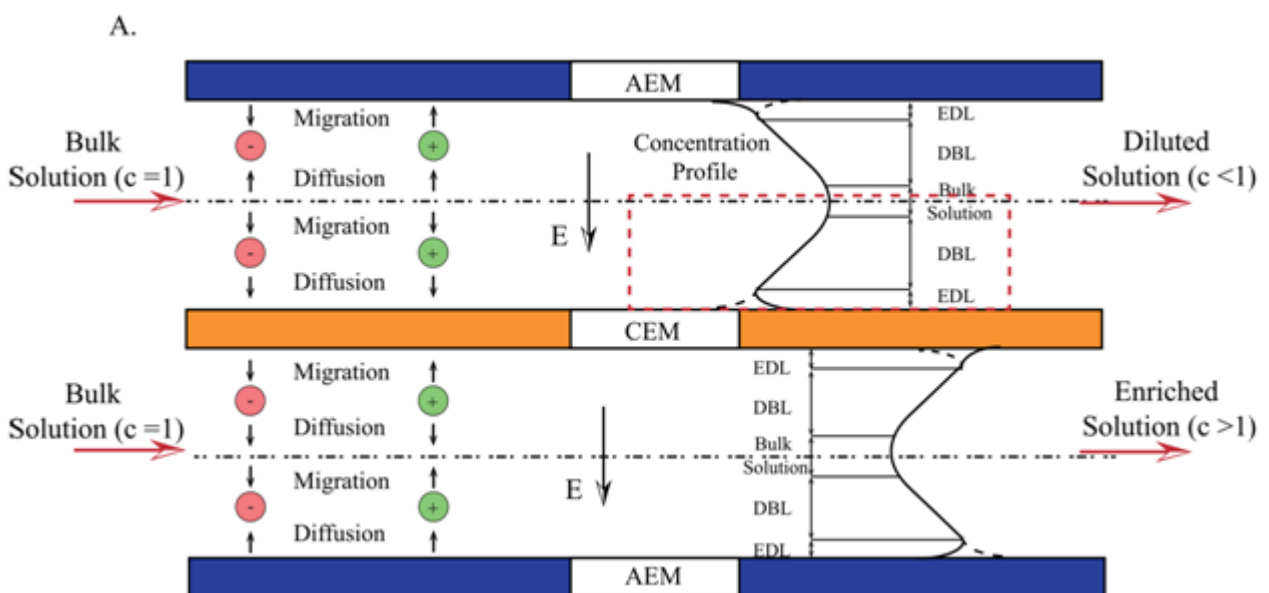
A. Nanochannel
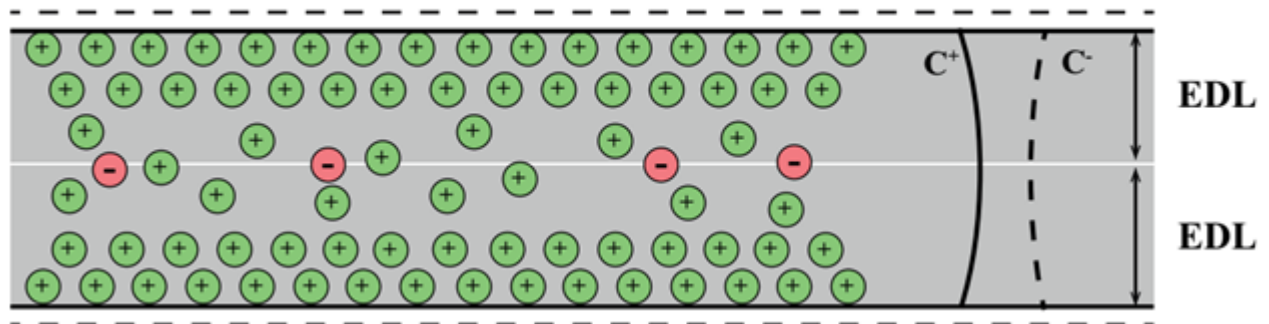
B. Microchannel

Figure 1: The thickness of the electrical double layer (EDL) is inversely proportional to the bulk concentration of the electrolyte solution. At low concentrations, thickness of the EDL will be in few nanometers. (A). shows the EDL from both sides of the nanochannel covers the entire nanochannel and screens the coions entering into it. (B). such a phenomenon is not observed in microchannel due to its larger dimension. The EDL remains local to the microchannel and bulk solution is maintained at the center

Fig. 1 The thickness of the electrical double layer (EDL) is inversely proportional to the bulk concentration of the electrolyte solution. At low concentrations, thickness of the EDL will be in few nanometers. (A). shows the EDL from both sides of the nanochannel covers the entire nanochannel and screens the coions entering into it. (B). such a phenomenon is not observed in microchannel due to its larger dimension. The EDL remains local to the microchannel and bulk solution is maintained at the center.
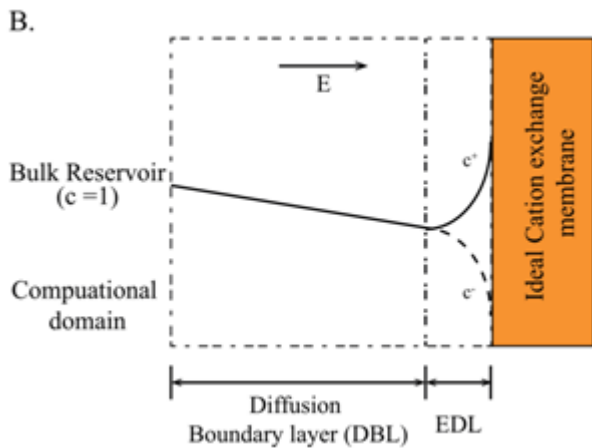
applications are modeled using Poisson-Nernst-Planck (PNP) equation.

$$\bar{C}_{it} = -\bar{\nabla}\underline{\bar{J}}_i \tag{1a}$$

$$\underline{\bar{J}}_i = \bar{v}\bar{C}_i - D_i\left(\bar{\nabla}\bar{C}_i + \frac{Fz_i\bar{C}_i}{RT}\bar{\nabla}\bar{\varphi}\right) \tag{1b}$$

$$\underline{\bar{j}}_i = -D_i\bar{\nabla}\bar{C}_i - \kappa_i z_i F\bar{C}_i\bar{\nabla}\bar{\varphi} \tag{1c}$$

$$\kappa_i = \frac{D_i}{RT} \tag{1d}$$

where $(\bar{.})$ refers to dimensional variable, $(\underline{.})$ refers vector quantity, $()_t$ is time derivative $(\partial()/\partial t)$, $\bar{\nabla}$ is laplacian operator, i refers to ionic species (i = 1,2,...M), $\bar{C}_i$ is concentration of species, D_i is ionic diffusivity, $\bar{\varphi}$ is electric potential, z_i is valance of the ion, $\bar{v}$ is the velocity vector, F is the Faraday constant, R is the universal gas constant, T is the Temperature, κ_i ionic mobility relates diffusivity by Einstein's relation Eq. (1d), the first term in the right side of the Eq. (1b) refers to the convection flux, $\underline{\bar{j}}$ refers to the electro-diffusion flux. The first term in Eq. (1c) is diffusional flux proportional to the concentration gradient $\bar{\nabla}\bar{C}_i$ and the second term is migration flux proportional to the potential gradient $\bar{\nabla}\bar{\varphi}$. To calculate the electric potential distribution we solve the electrostatic Poisson equation which is given by,

$$d\bar{\nabla}^2\bar{\varphi} = -4\pi\bar{\rho}_e \tag{2a}$$

here, d is the relative permittivity and is given by,

$$d = \epsilon_r\epsilon_o \tag{2b}$$

Figure 2: (A) The schematic representation of the classical electrodialysis cell. The concentration gradients or salinity gradients are created on the both sides of the membrane due to the applied electric field. This phenomenon is known as ion concentration polarization (ICP). Due to the ICP phenomena the diluted and concentrated solutions are produced at the top and bottom interface of CEM, respectively. (B) The computational domain of the CEM or AEM or IEM in general used in the literature is shown

3. Theory and Computational Simulations of IEM Membrane Technology

The ions and fluid transport is studied predominantly as the solids/gases transport are well understood transport technology with the advancements in electronics and aircraft industries in the last century technology advancements. The ions and fluid transport, in membrane technology

ϵ_r is the relative permittivity of the medium, ϵ_o is the permittivity of the free space, $\bar{\rho}$ is the space charge density reads,

$$\bar{\rho}_e = \sum_{i=1}^{M} z_i F\bar{C}_i \tag{2c}$$

Total ionic current reads

$$\bar{I} = \sum_{i=1}^{M} Fz_i\underline{\bar{J}}_i \tag{3}$$

To find the velocity vector $\underline{\bar{v}}$, the Navier-Stokes equation of fluid flow by assuming viscous Newtonian fluid and continuity equation is given by,

$$\rho\left(\underline{\bar{v}}_t + \underline{\bar{v}}\bar{\nabla}\underline{\bar{v}}\right) = -\bar{\nabla}\bar{p} + \underline{\bar{\phi}}_e + \mu\bar{\nabla}^2\underline{\bar{v}} \tag{4a}$$

where ρ is the solution density, $\bar{p}$ is the pressure, μ is the dynamic viscosity. $\underline{\bar{\phi}}_e$ is the electrostatic body force. The continuity equation is given by,

$$\bar{\nabla}.\underline{\bar{v}} = 0 \tag{4b}$$

And boundary conditions are given by,

$$c^+|_{y=0} = c^-|_{y=0} = 1, \quad \varphi|_{y=0} = 0 \tag{5a}$$

$$c^+|_{y=1} = N, \quad \left(\frac{dc^-}{dy} + c^-\frac{d\varphi}{dy}\right)\Big|_{y=1} = 0 \quad \varphi|_{y=1} = -V \tag{5b}$$

And the fluid transport is determined from the Navier-Stokes equations, mentioned earlier using 1D approximation analytical solutions for Stokes equation.

4. Experimental Observations of IEM Membrane Technology Ions/Fluid Transport

For a IEM with wavy or a V-type geometry membrane technology, Rubinstein's early works [72], Pham and Han et al. [73] recent works observed two dimensional fluid motion with fluid vortice structures in Fig. 3 were observed. The experimental observations for fluid, ions transport and the resulting current-voltage measurements for energy applications, showed in Fig. 4, [47, 50, 62, 76-78] further showcased the nonlinear fluid, ion and current-voltage measurements in IEM membrane technology.
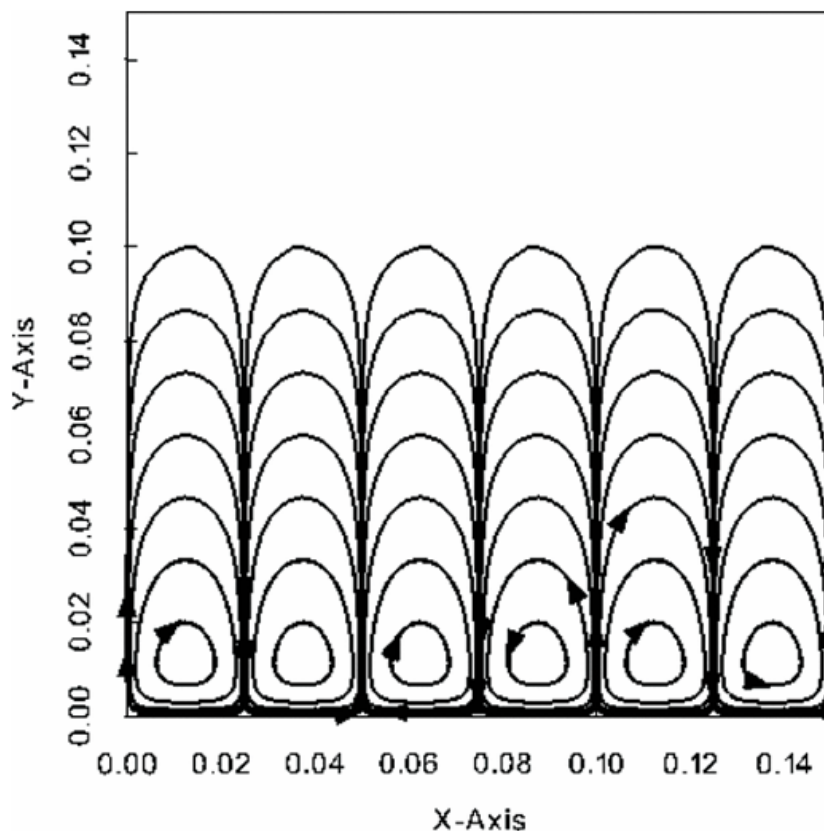

Figure 3: The seed vortices reprinted with permission from [73] copyright 2012 by the American Physical Society
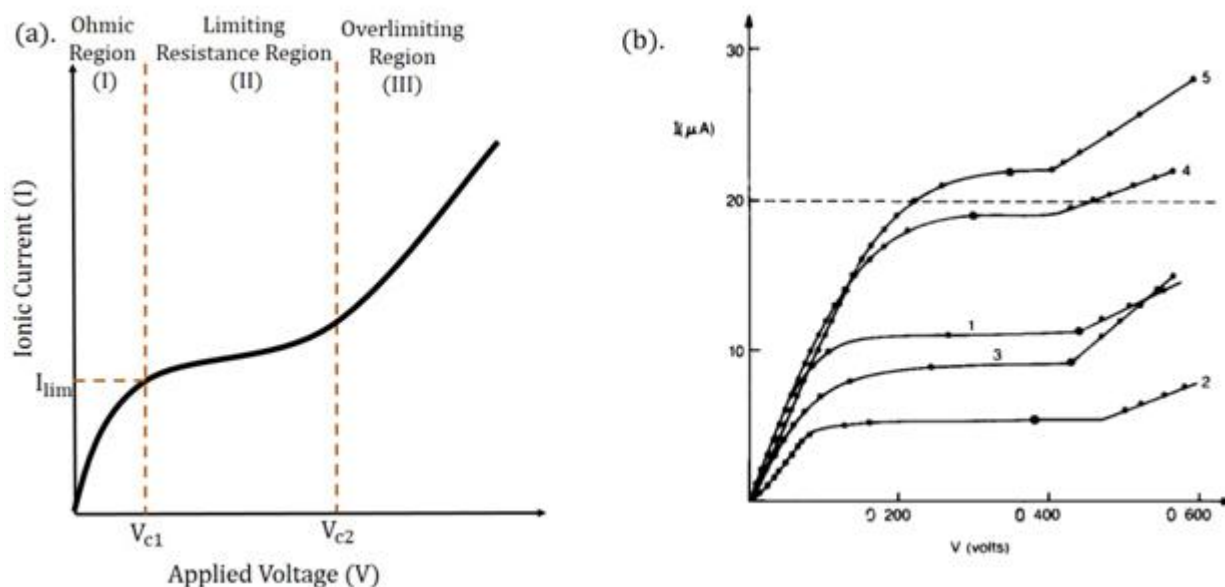

Figure 4: (A) Schematic representation of nonlinear current-voltage measurement in IEM membrane technology (B) Experimental current-voltage measurement in IEM membrane technology. Reprinted with permission from [63] copyright 1988 by Elesvier.

The earlier theoretical and computational modeling did not explain the experimental observations which left lot of experimental observations fully not explainable to applications of membrane technology where IEM are used. Owing to the incomplete theoretical and computational modeling, many plausible explanations were given for the

nonlinear current-voltage measurement in IEM, deviations from Ohmic current, with current limiting and again over increasing again after the limiting regime, having an overlimiting regime. Additional charge carriers due to water splitting, gravitational convection, electroconvection, electroosmosis, fluidic and electroconvective instabilities were believed to be the mechanisms behind the nonlinear current-voltage measurement in IEM. The dashed line in Fig. 5 (A)-(C) represents the surface of the CEM[78]. Fig. 5.(D) shows the Ohmic region (represented by I) with no electroosmotic flow followed by the limiting resistance region (region II), then the size of the electroosmotic flow vortex grows with time and voltage.
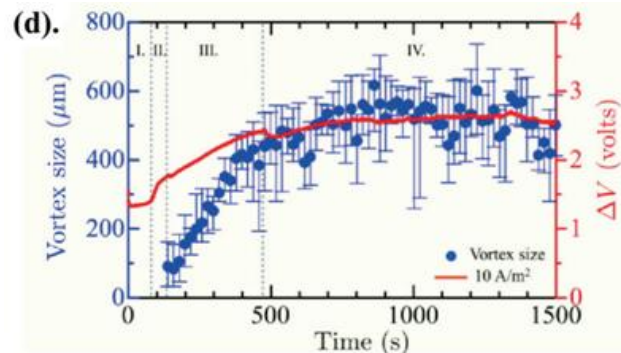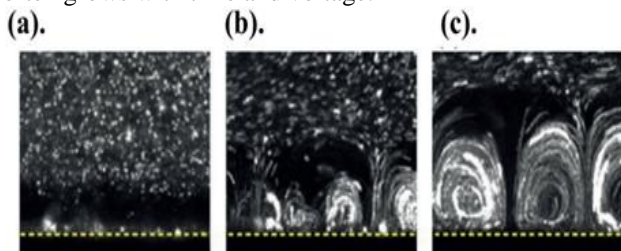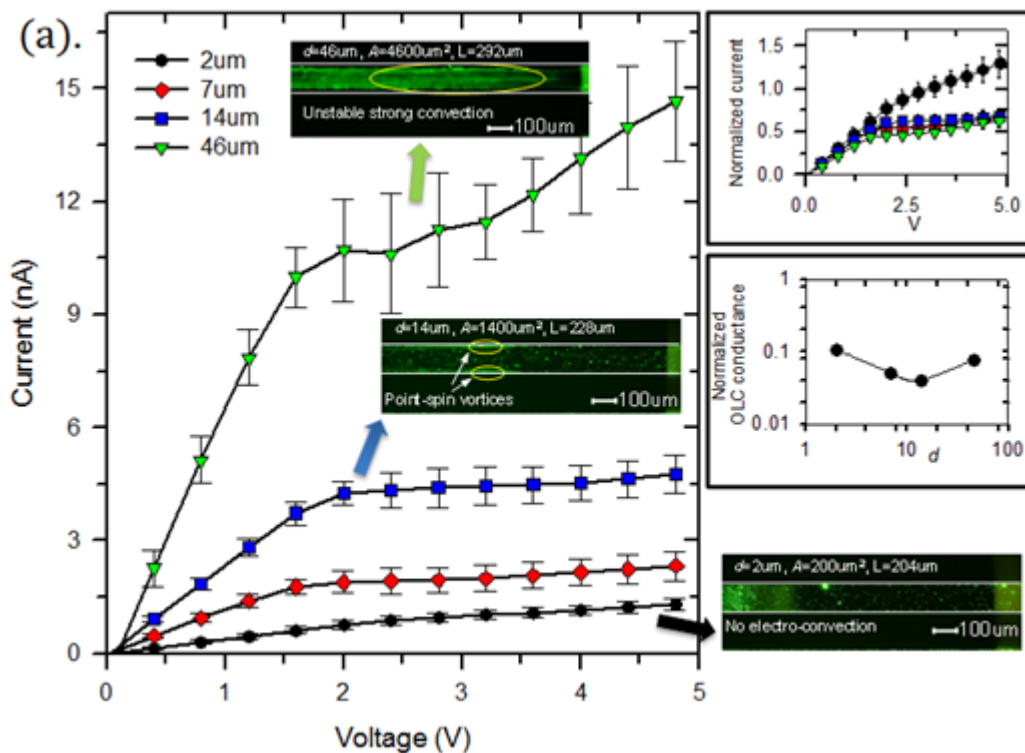

Figure 5: (A)-(C). The nonlinear electroosmotic flow near CEM (D) Variation of the size of the vortices with the applied voltage and time. Reprinted with permission from [78] copyright 2015 by the American Physical Society.

Fig. 6 shows the nonlinear current-voltage measurement observation and nonlinear electroosmotic flow near CEM, region, of four different channel depths, experiments performed with. Experiments by Pu et al.[32] demonstrated the enrichment-depletion region concentration fluorescent image, inside a micro/nanofluidic membrane technology applications. Fig. 7 shows the Rhodamine 6G fluorescent in 100mM phosphate buffer and 70mM phosphate buffer, depletion and enrichment regions.
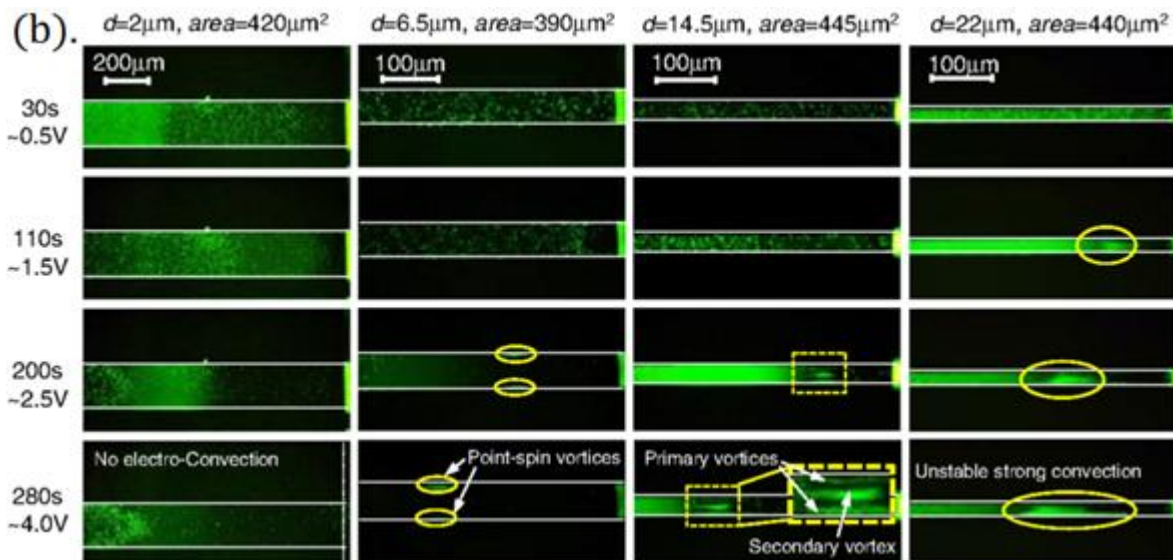
Figure 6: (A) Nonlinear current-voltage measurement, in CEM membrane technology of four different channel depths (B) The experimental observation of nonlinear electroosmotic flow near IEM, region. Reprinted with permission from [78] copyright 2015 by the American Physical Society.
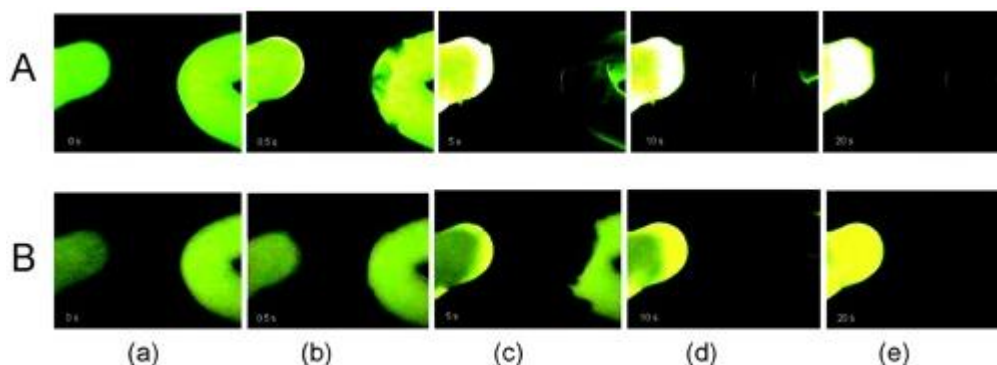

Figure 7: Experimental observations of concentration fluorescent images of (A) Rhodamine 6G in 100mM phosphate buffer, image visualization for depletion region at (a-e) 0,0.5,5,10,20s. (B) Rhodamine 6G in 70mM phosphate buffer, image visualization for enrichment region at (a-e) 0,0.5,5,10,20s in micro/nanofluidic membrane technology applications. Reprinted with permission from [32] copyright 2004 by the American Chemical Society.

Kim and Han et al.[37] showed nonlinear current-voltage measurement across a micro/nanofluidic membrane technology applications and the fluorescent image visualization of the depletion and enrichment regions (see Fig. 8) for a micro/nanofluidic membrane technology. Yossifon and Chang [40,41] in their experiments showed electroconvective ion instability image visualization across their micro/nanofluidic membrane technology applications. Fig. 9 shows the frequency imaging visualization approach of imaging for electroconvective ion instability.
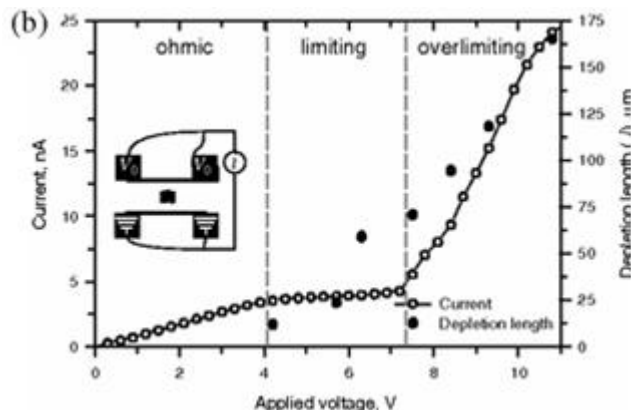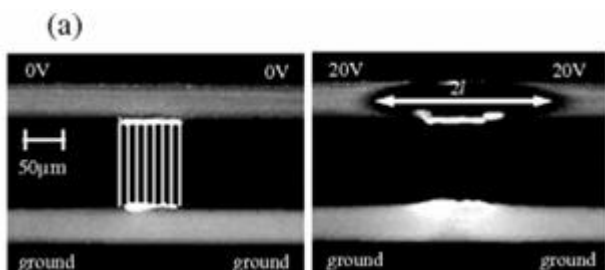

Figure 8: (A) Experimental fluorescene image visualization of depletion and enrichment region (B) nonlinear current-voltage measurement for micro/nanofluidic membrane technology applications. Reprinted with permission from [37] copyright 2007 by the American Physical Society.
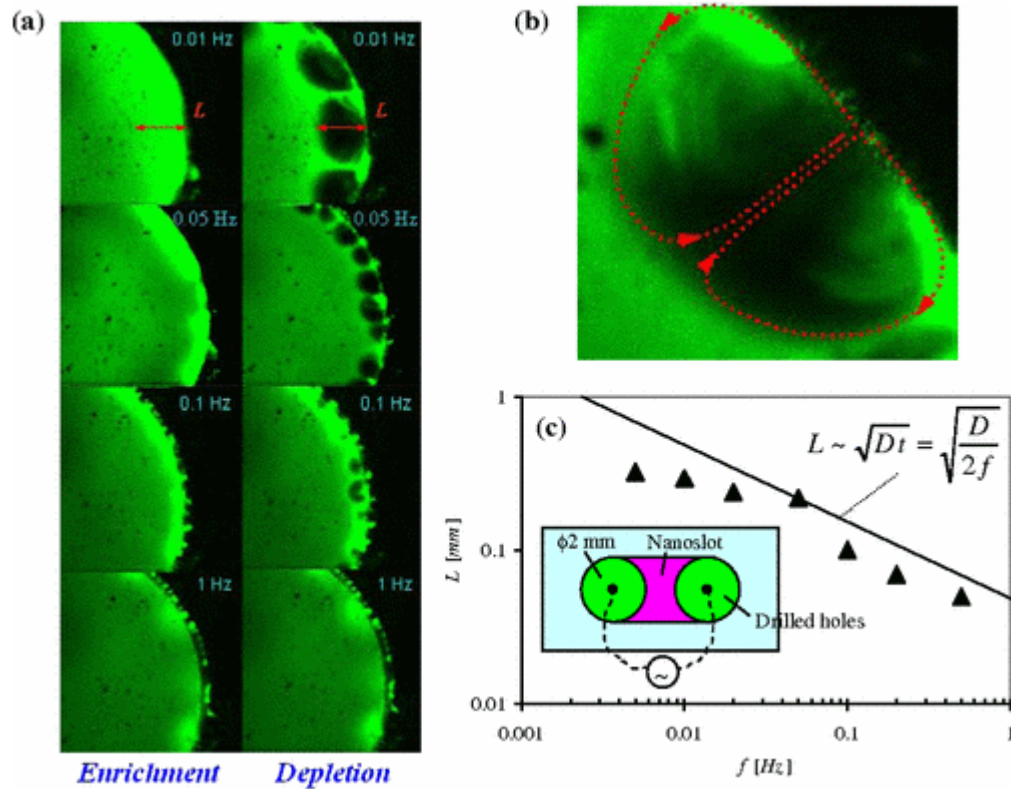
Figure 9: (A-C) Frequency imaging visualization of electroconvective ion instability in micro/nanofluidic membrane technology applications. Reprinted with permission from [40] copyright 2008 by the American Physical Society

Nandigana and Aluru [79] built a 2D computational model and package in OpenFOAM, open source platform, to simulate Poisson-Nernst-Planck and Navier-Stokes equations across a full micro/ nanofluidic membrane technology application use. The computer simulations of Nandigana et al. showed experimental observation of nonlinear current-voltage results with the mechanism that charge redistribution near the depletion region without nonlinear electroosmotic flow is the true mechnanism for the overlimiting current behavior as they had observed the nonlinear current-voltage result even when the fluid

contribution is switched off, considering only the contribution of ionic electrolyte solid powder in their computational simulations. Further, when the charge redistributes, the nonlinear current-voltage results are observed with no instability in the ions, but the charge redistributes with nonlinear electroconvection and charge redistribution was found to be the true mechanism of nonlinear current-voltage observations in experiments of membrane technology applications (see Fig. 10).
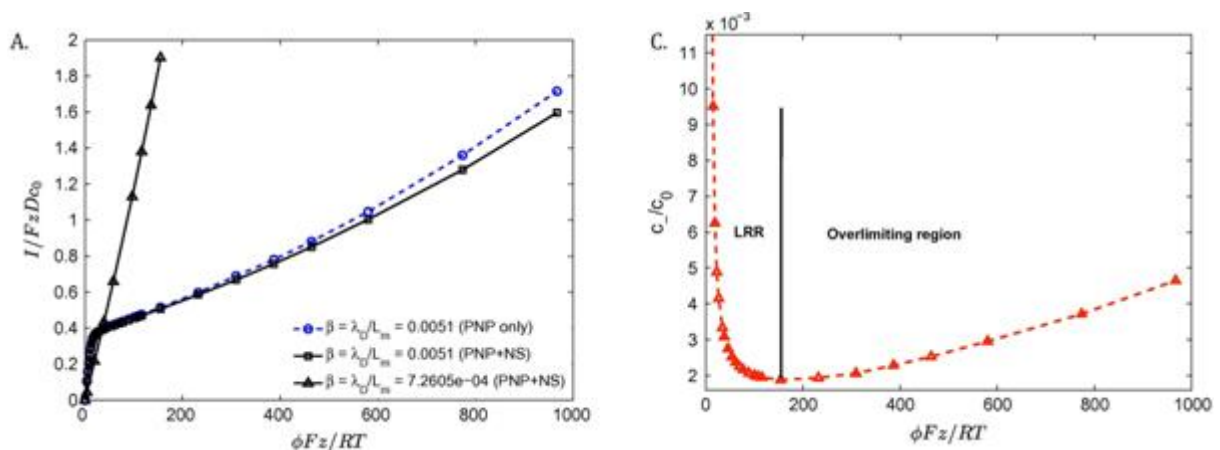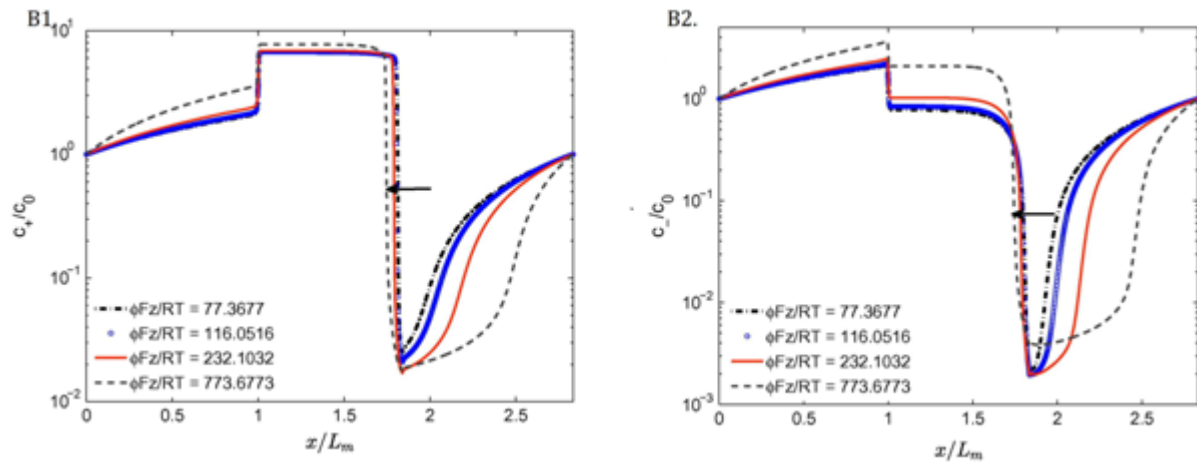
Figure 10: (A-C). Computational simulation of nonlinear current-voltage result with charge redistribution mechanism of ion concentration distribution across a micro/nanofluidic membrane technology application use. Reprinted with permission from [79] copyright 2012 by Elsevier

Further, in a follow up work, Nandigana et al.[80] proposed a nondimensional Nandigana number and a theoretical oscillator model, that predicts the onset of ion instability across a micro/nanofluidic membrane technology application. The nondimensional Nandigana number relates the surface charge density of the nanofluidic channel and the bulk electroconvection contribution given by,

$$N_n = \frac{\sigma ds}{4\pi \epsilon_0 \epsilon_r x V} \qquad (6)$$

where, σ is the surface charge density of the nanofluidic channel, V is the applied voltage, x is the characteristic bulk electroconvective EDL range dimension, usually few nanometers. The ion instability was found to occur in micro/nanofluidic membrane technology application, for Nandigana number greater than 0.05294, see Fig. 11 confirmed from computer simulations and theoretical model.
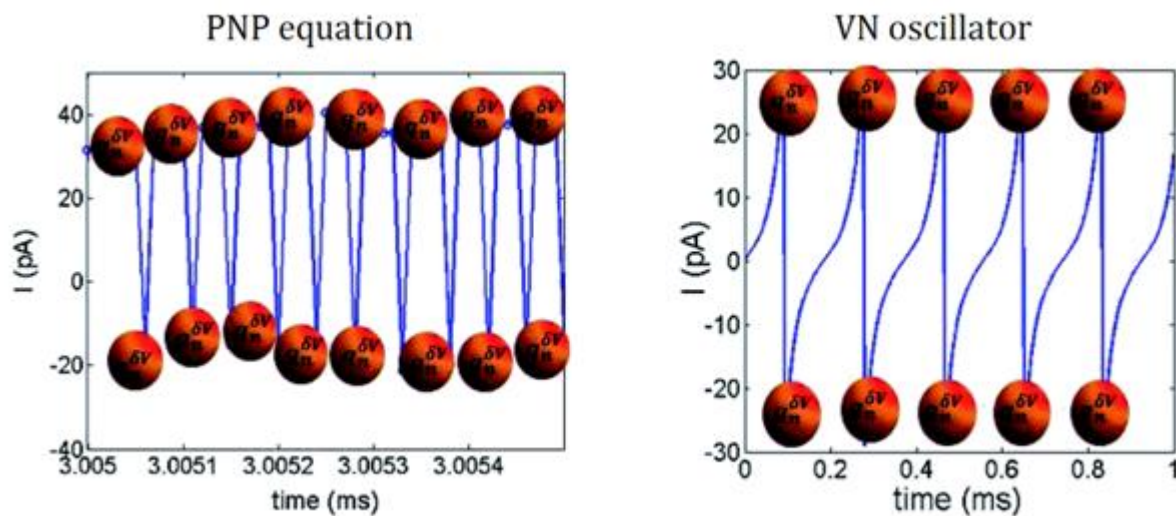

Figure 11: Ion instability computer simulation across a micro/nanofluidic membrane technology application with current instability results and comparison with theoretical oscillator model. Reprinted with permission from [80] copyright 2017 by the Royal Society of Chemistry

To reconfirm the mechanism of charge redistribution for nonlinear current-voltage measurements in membrane technology applications use, Nandigana et al.[81] built a 2D computational model and package in OpenFOAM, open source platform, to simulate Poisson-Nernst-Planck and Navier-Stokes equations for electrochemical impedance spectroscopy (EIS), AC measurements across a full micro/nanofluidic membrane technology application use.

Fig. 12 shows the Nyquist impedance result ($-\text{lm}(Z)$ vs $\text{Re}(Z)$) showing the transition from resistance-capacitance charge dynamics to resistance-capacitance-inductance charge dynamics on the trigger of nonlinear current-voltage results confirming the charge redistribution of ions as the true mechanism for nonlinear current-voltage results across membrane technology applications.
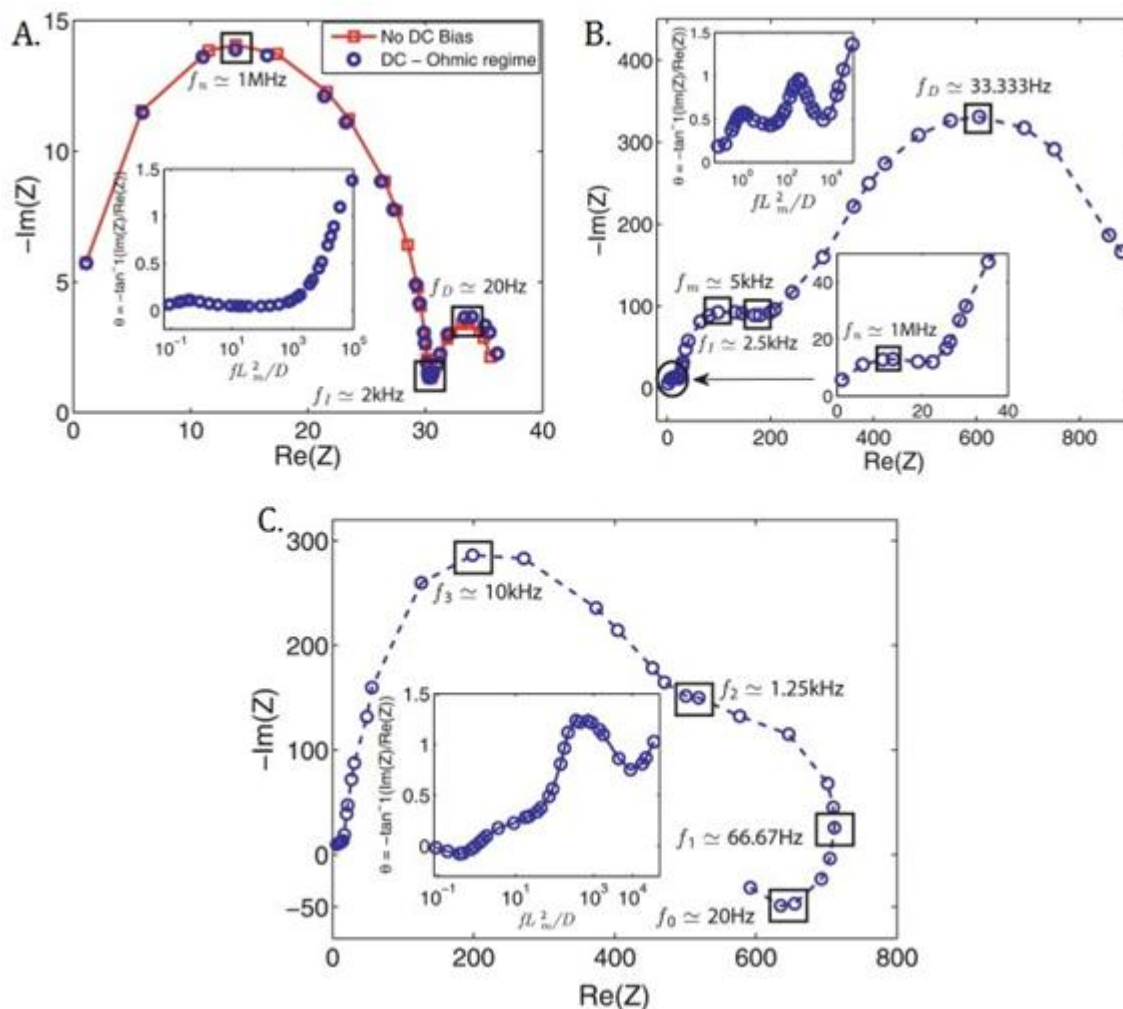
Figure 12: 12. (A-C) Computer simulation of Electrochemical Impedance Spectroscopy (EIS), with Nyquist impedance result showing transition from resistance-capacitance charge dynamics to resistance-capacitance-inductance charge dynamics on the trigger of nonlinear current-voltage results across membrane technology applications. Reprinted with permission from [81] copyright 2013 by Elsevier

5. Conclusion

Here, we provide a detailed literature review on membrane technology, IEMs and micro/nanofluidic membrane applications, membrane technology physics, science, theory, computational simulations, experiments review literature for the last three decades for membrane technology use in energy, safe drinking water supply and production, that is environmentally green friendly and compatible with the natural resources in its production and usage, ionic circuits, fluidic electronics, membrane technology for faster transport of solids/liquids/gases/mixtures of using membrane technology for pipeline construction industry and use in humankind of 2021 era.

6. Acknowledgements

7. Conflict of Interest

The authors have declared no conflict of interest.

References

[1] K. Mani, Electrodialysis water splitting technology, Journal of Membrane Science 58 (1991) 117 – 138.
[2] H. Bishop, J. Bittles, G. Guter, Investigation of inorganic ion exchange membranes for electrodialysis, Desalination 6 (1969) 369 – 380.
[3] T. Sata, T. Sata, W. Yang, Studies on cation-exchange membranes having permselectivity between cations in electrodialysis, Journal of Membrane Science 206 (2002) 31 – 60.
[4] T. Sata, Studies on anion exchange membranes having permselectivity for specific anions in electrodialysis - effect of hydrophilicity of anion exchange membranes on permselectivity ljf anions, Journal of Membrane Science 167 (2000) 1 – 31.
[5] T. Morimoto, M. Yoshitake, S. Morikawa, Y. Oda, Alkaline type ion-exchange membrane water electrolysis, International Journal of Hydrogen Energy 11 (1986) 503 – 506.

[6] M. K. Cho, H.-Y. Park, S. Choe, S. J. Yoo, J. Y. Kim, H.-J. Kim, D. Henkensmeier, S. Y. Lee, Y.-E. Sung, H. S. Park, J. H. Jang, Factors in electrode fabrication for performance enhancement of anion exchange membrane water electrolysis, Journal of Power Sources 347 (2017) 283 – 290.

[7] L. A. Diaz, T. E. Lister, C. Rae, N. D. Wood, Anion exchange membrane electrolyzers as alternative for upgrading of biomass-derived molecules, ACS Sustainable Chemistry & Engineering 6 (2018) 8458–8467.

[8] H. Ito, N. Kawaguchi, S. Someya, T. Munakata, N. Miyazaki, M. Ishida, A. Nakano, Experimental investigation of electrolytic solution for anion exchange membrane water electrolysis, International Journal of Hydrogen Energy 43 (2018) 17030 – 17039.

[9] H. Ito, N. Kawaguchi, S. Someya, T. Munakata, Pressurized operation of anion exchange membrane water electrolysis, Electrochimica Acta 297 (2019) 188 – 196.

[10] J. E. Park, S. Y. Kang, S.-H. Oh, J. K. Kim, M. S. Lim, C.-Y. Ahn, Y.-H. Cho, Y.-E. Sung, High-performance anion-exchange membrane water electrolysis, Electrochimica Acta 295 (2019) 99 – 106.

[11] G. Merle, M. Wessling, K. Nijmeijer, Anion exchange membranes for alkaline fuel cells: A review, Journal of Membrane Science 377 (2011) 1 – 35.

[12] Y. Zhao, H. Yu, D. Yang, J. Li, Z. Shao, B. Yi, High-performance alkaline fuel cells using crosslinked composite anion exchange membrane, Journal of Power Sources 221 (2013) 247 17– 251.

[13] D. R. Dekel, Review of cell performance in anion exchange membrane fuel cells, Journal of Power Sources 375 (2018) 158 – 169.

[14] Z. Pan, L. An, T. Zhao, Z. Tang, Advances and challenges in alkaline anion exchange membrane fuel cells, Progress in Energy and Combustion Science 66 (2018) 141 – 175.

[15] V. Vijayakumar, S. Y. Nam, Recent advancements in applications of alkaline anion exchange membranes for polymer electrolyte fuel cells, Journal of Industrial and Engineering Chemistry 70 (2019) 70 – 86.

[16] J. C. T. Eijkel, A. v. d. Berg, Nanofluidics: what is it and what can we expect from it?, Microfluidics and Nanofluidics 1 (2005) 249–267.

[17] R. Mukhopadhyay, What does nanofluidics have to offer?, Analytical Chemistry. 78 (2006) 7379–7382.

[18] R. B. Schoch, J. Han, P. Renaud, Transport phenomena in nanofluidics, Rev. Mod. Phys. 80 (2008) 839–883.

[19] M. Ventra, S. Evoy, J. R. Heflin, Introduction to nanoscale science and technology, Nanostructure Science and Technology. 1 (2008).

[20] L. Bocquet, E. Charlaix, Nanofluidics, from bulk to interfaces, Chem. Soc. Rev 39 (2010) 1073–1095.

[21] Y. Xu, Nanofluidics: A new arena for materials science, Advanced Materials. 30 (2018) 1702419.

[22] I. Vlassiouk, S. Smirnov, Z. Siwy, Ionic selectivity of single nanochannels, Nano Letters 8 (2008) 1978–1985.

[23] J. Cervera, B. Schiedt, R. Neumann, S. Mafe, P. RamÃrez, Ionic conduction, rectification, and selectivity in single conical nanopores, The Journal of Chemical Physics 124 (2006) 104706.

[24] R. Karnik, R. Fan, M. Yue, D. Li, P. Yang, A. Majumdar, Electrostatic control of ions and molecules in nanofluidic transistors, Nano Letters 5 (2005) 943–948.

[25] P. M. Biesheuvel, P. Stroeve, P. A. Barneveld, Effect of protein adsorption and ionic strength on the equilibrium partition coefficient of ionizable macromolecules in charged nanopores, The Journal of Physical Chemistry B 108 (2004) 17660–17665.

[26] P. Ramirez, S. Mafe, A. Alcaraz, J. Cervera, Modeling of ph switchable ion transport and selectivity in nanopore membranes with fixed charges, The Journal of Physical Chemistry B 107 (2003) 13178–13187.

[27] S. H. Behrens, M. Borkovec, Electrostatic interaction of colloidal surfaces with variable charge, The Journal of Physical Chemistry B 103 (1999) 2918–2928.

[28] H. Daiguji, P. Yang, A. Majumdar, Ion transport in nanofluidic channels, Nano Letters 4 (2004) 137–142.

[29] C. Dekker, Solid-state nanopores, Nature Nanotechnology 2 (2007) 209.

[30] M. Tagliazucchi, I. Szleifer, Transport mechanisms in nanopores and nanochannels: can we mimic nature?, Materials Today 18 (2015) 131 – 142.

[31] M. Mao, S. Ghosal, G. Hu, Hydrodynamic flow in the vicinity of a nanopore induced by an applied voltage, IOP Publishing 24 (2013) 245202.

[32] Q. Pu, J. Yun, H. Temkin, S. Liu, Ion-enrichment and ion-depletion effect of nanochannel structures., Nano Lett. 4 (2004) 1099.

[33] A. Datta, S. Gangopadhyay, H. Temkin, Q. Pu, S. Liu, Nanofluidic channels by anodic bonding of amorphous silicon to glass to study ion-accumulation and ion-depletion effect, Talanta 68 (2006) 659 – 665.

[34] R. Dhopeshwarkar, R. M. Crooks, D. Hlushkou, U. Tallarek, Transient effects on microchannel electrokinetic filtering with an ion-permselective membrane, Analytical Chemistry 80 (2008) 1039.

[35] D. Hlushkou, R. Dhopeshwarkar, R. M. Crooks, U. Tallarek, The influence of membrane ion-permselectivity on electrokinetic concentration enrichment in membrane-based preconcentration units, Lab Chip 8 (2008) 1153–1162.

[36] K. Zhou, M. L. Kovarik, S. C. Jacobson, Surface-charge induced ion depletion and sample stacking near single nanopores in microfluidic devices, Journal of the American Chemical Society 130 (2008) 8614.

[37] S. J. Kim, Y.-C. Wang, J. H. Lee, H. Jang, J. Han, Concentration polarization and nonlinear electrokinetic flow near nanofluidic channel, Phys. Rev. Lett. 99 (2007) 044501.

[38] S. J. Kim, J. Han, Self-sealed vertical polymeric nanoporous-junctions for high-throughput nanofluidic applications, Analytical Chemistry 80 (2008) 3507.

[39] S. J. Kim, L. D. Li, J. Han, Amplified electrokinetic response by concentration polarization near nanofluidic channel, Langmuir 25 (2009) 7759.

[40] G. Yossifon, H.-C. Chang, Selection of nonequilibrium overlimiting currents: Universal depletion layer formation dynamics and vortex instability, Phys. Rev. Lett. 101 (2008) 254501

[41] H.-C. Chang, G. Yossifon, E. A. Demekhin, Nanoscale electrokinetics and microvortices: How microhydrodynamics affects nanofluidic ion flux, Annual Review of Fluid Mechanics 44 (2012) 401–426.

[42] M. Li, R. K. Anand, Recent advancements in ion concentration polarization, Analyst 141 (2016) 3496–3510.

[43] S. Y. Park, C. J. Russo, D. Branton, H. A. Stone, Eddies in a bottleneck: An arbitrary debye length theory for capillary electroosmosis, Journal of Colloid and Interface Science 297 (2006) 832 – 839.

[44] T. Postler, Z. Slouka, M. Svoboda, M. Pribyl, D. Snita, Parametrical studies of electroosmotic transport characteristics in submicrometer channels, Journal of Colloid and Interface Science 320 (2008) 321 – 332.

[45] N. W. Rosenberg, C. E. Tirrell, Limiting currents in membrane cells, Industrial & Engineering Chemistry 49 (1957) 780–784.

[46] D. A. Cowan, J. H. Brown, Effect of turbulence on limiting current in electrodialysis cells, Industrial & Engineering Chemistry 51 (1959) 1445–1448.

[47] B. Cooke, Concentration polarization in electrodialysis I. the electrometric measurement of interfacial concentration, Electrochimica Acta 3 (1961) 307 – 317.

[48] V. G. Levich, Physicochemical hydrodynamics, Prentice-Hall, N.Y. (1962) 242.

[49] H. P. Gregor, M. A. Peterson, Electrodialytic polarization of ion-exchange membrane systems, The Journal of Physical Chemistry 68 (1964) 2201–2205.

[50] T. Yamabe, M. Seno, The concentration polarization effect in ion exchange membrane electrodialysis, Desalination 2 (1967) 148 – 153.

[51] H. F. Weber, Untersuchungen Ã ber das elementargesetz der hydrodiffusion, Annalen der Physik 243 (1879) 536–552.

[52] R. D. Patel, K.-C. Lang, I. F. Miller, Polarization in ion-exchange membrane electrodialysis, Industrial & Engineering Chemistry Fundamentals 16 (1967) 340–348.

[53] K. Spiegler, Polarization at ion exchange membrane-solution interfaces, Desalination 9 (1971) 367 – 385.

[54] C. Forgacs, N. Ishibashi, J. Leibovitz, J. Sinkovic, K. Spiegler, Polarization at ion-exchange membranes in electrodialysis, Desalination 10 (1972) 181 – 214.

[55] M. Metayer, C. Bourdillon, E. Selegny, Concentration polarization on ion-exchange membranes in electrodialysis with natural convection:: Estimating interfacial concentrations by measurement of membrane potential decay caused by concentration relaxation after current cut-off, Desalination 13 (1973) 129 – 146.

[56] O. Kedem, Reduction of polarization in electrodialysis by ion-conducting spacers, Desalination 16 (1975) 105 – 118.

[57] B. Gavish, S. Lifson, Membrane polarisation at high current densities, J. Chem. Soc., Faraday Trans. 1 75 (1979) 463–472.

[58] I. Rubinstein, L. Shtilman, Voltage against current curves of cation exchange membranes, J. Chem. Soc., Faraday Trans. 2 75 (1979) 231–246.

[59] O. Kedem, I. Rubinstein, Polarization effects at charged membranes, Desalination 46 (1983) 185–189.

[60] Y. Tanaka, M. Seno, Concentration polarization and water dissociation in ion-exchange membrane electrodialysis. mechanism of water dissociation, J. Chem. Soc., Faraday Trans. 1 82 (1986) 2065–2077.

[61] Y. I. Kharkats, The mechanism of supralimiting currents at ion-exchange membrane electrolyte interfaces, Sov. Electrochem. (Engl. Transl.); (United States) (1986).

[62] I. Rubinstein, E. Staude, O. Kedem, Role of the membrane surface in concentration polarization at ion-exchange membrane, Desalination 69 (1988) 101 – 114.

[63] I. Rubinstein, Electro-diffusion of ions, society of industrial and applied mathematics (1990).

[64] Y. Tanaka, Concentration polarization in ion exchange membrane electrodialysis, Journal of Membrane Science 57 (1991) 217 – 235.

[65] V. Shaposhnik, V. Vasil'eva, D. Praslov, Concentration fields of solutions under electrodialysis with ion-exchange membranes, Journal of Membrane Science 101 (1995) 23 – 30.

[66] I. Rubinstein, B. Zaltzman, Electrodiffusional free boundary problem in concentration polarization in electrodialysis, Mathematical Models and Methods in Applied Sciences 06 (1996) 623–648.

[67] J. A. Manzanares, W. D. Murphy, S. Mafe, H. Reiss, Numerical simulation of the nonequilibrium diffuse double layer in ion-exchange membranes, The Journal of Physical Chemistry 97 (1993) 8524.

[68] T. Xu, W. Yang, Fundamental studies on a novel series of bipolar membranes prepared from poly(2,6−dimethyl−1,4−phenylene oxide) (ppo): I. effect of anion exchange layers on i−v curves of bipolar membranes, Journal of Membrane Science 238 (2004) 123 – 129.

[69] F. C. Leinweber, U. Tallarek, Nonequilibrium electrokinetic effects in beds of ionpermselective particles, Langmuir 20 (2004) 11637–11648.

[70] S. J. Lee, J. Lee, K. Kim, Pressure-driven spontaneous ion concentration polarization using an ion-selective membrane, Analytical Biochemistry 557 (2018) 13 – 17.

[71] H. Lee, D. Kim, J. Y. Kang, K. W. Bong, S. H. Lee, R. Kwak, Nonlinear dynamics of ion concentration polarization in capacitive deionization, Desalination 458 (2019) 14 – 24.

[72] I. Rubinstein, B. Zaltzman, Electro-osmotically induced convection at a permselective membrane, Phys. Rev. E 62 (2000) 2238–2251.

[73] V. S. Pham, Z. Li, K. M. Lim, J. K. White, J. Han, Direct numerical simulation of electroconvective instability and hysteretic current-voltage response of a permselective membrane, Phys. Rev. E. 86 (2012) 046310.

[74] F. Maletzki, H. Rosler, E. Staude, Ion transfer across electrodialysis membranes in the overlimiting current range: stationary voltage current characteristics and current noise power spectra under different conditions of free convection, Journal of Membrane Science 71 (1992) 105 – 116.

[75] V. Zabolotsky, V. Nikonenko, N. Pismenskaya, E. Laktionov, M. Urtenov, H. Strathmann, M. Wessling, G. Koops, Coupled transport phenomena in overlimiting current electrodialysis, Separation and Purification Technology. 14 (1998) 255 – 267.

[76] M. Block, J. A. Kitchener, Polarization phenomena in commercial ion-exchange membranes, Journal of the Electrochemical Society 113 (1996) 947–953.

[77] J. C. de Valença, R. M. Wagterveld, R. G. H. Lammertink, P. A. Tsai, Dynamics of microvortices induced by ion concentration polarization, Phys. Rev. E 92 (2015) 031003.

[78] S. Nam, I. Cho, J. Heo, G. Lim, M. Z. Bazant, D. J. Moon, G. Y. Sung, S. J. Kim, Experimental verification of overlimiting current by surface conduction and electroosmotic flow in microchannels, Phys. Rev. Lett. 14 (2015) 114501.

[79] V.V. R. Nandigana, N. R. Aluru, Understanding anomalous current−voltage characteristics in microchannel−nanochannel interconnect devices, J. Colloid Interface Sci. 384 (2012) 162.

[80] V.V.R. Nandigana, N. R. Aluru, 1/f pink chaos in nanopores, RSC Adv. 7 (2017) 46092–46100.

[81] V.V.Nandigana, N. R. Aluru, Characterization of electrochemical properties of a micronanochannel integrated system using computational impedance spectroscopy (cis), Electrochimica Acta 105 (2013) 514 – 523.